Earth's Future

RESEARCH ARTICLE
10.1029/2024EF004736

Special Collection:
Past and Future of Marine Ecosystems

Assessing the Time of Emergence of Marine Ecosystems From Global to Local Scales Using IPSL-CM6A-LR/APECOSM Climate-To-Fish Ensemble Simulations

Nicolas Barrier[1], Olivier Maury[1], Roland Seferian[2], Yeray Santana-Falcón[3], Alex Tidd[1], and Matthieu Lengaigne[1]

[1]MARBEC, University Montpellier, CNRS, Ifremer, IRD, Sète, France, [2]CNRM, Université de Toulouse, Météo-France, CNRS, Toulouse, France, [3]Instituto de Oceanografía y Cambio Global, Universidad de Las Palmas de Gran Canaria, Telde, Spain

Key Points:

- The Time of Emergence (ToE) of the marine ecosystem is investigated for the first time using ensemble climate-to-fish simulations
- Emergence of fish biomass is driven by the concentration of lower trophic levels and modulated by temperature through trophic amplification
- The ToE pattern closely follows the signal-to-noise ratio, which is mostly influenced by the strength of the climate change signal

Supporting Information:

Supporting Information may be found in the online version of this article.

Correspondence to:

N. Barrier,
nicolas.barrier@ird.fr

Citation:

Barrier, N., Maury, O., Seferian, R., Santana-Falcón, Y., Tidd, A., & Lengaigne, M. (2025). Assessing the time of emergence of marine ecosystems from global to local scales using IPSL-CM6A-LR/APECOSM climate-to-fish ensemble simulations. *Earth's Future*, *13*, e2024EF004736. https://doi.org/10.1029/2024EF004736

Received 27 MAR 2024
Accepted 15 JAN 2025

Abstract Climate change is anticipated to considerably reduce global marine fish biomass, driving marine ecosystems into unprecedented states with no historical analogs. The Time of Emergence (ToE) marks the pivotal moment when climate conditions (i.e., signal) deviate from pre-industrial norms (i.e., noise). Leveraging ensemble climate-to-fish simulations from one Earth System Model (IPSL-CM6A-LR) and one Marine Ecosystem Model (APECOSM), this study examines the ToE of epipelagic, migratory and mesopelagic fish biomass alongside their main environmental drivers for two contrasted climate-change scenarios. Globally averaged biomass signals emerge over the historical period. Epipelagic biomass decline emerged earlier (1950) than mesozooplankton decline (2017) due to a stronger signal in the early 20th century, possibly related to trophic amplification induced by an early emerging surface warming (1915). Trophic amplification is delayed for mesopelagic biomass due to postponed warming in the mesopelagic zone, resulting in a later emergence (2017). ToE also displays strong size class dependence, with epipelagic medium sizes (20 cm) experiencing delayed emergence compared to the largest (1 m) and smallest (1 cm) categories. For the epipelagic and mesopelagic communities, the regional signal emergence lags behind the global average, with median ToE estimates of 2030 and 2034, respectively. This is due to stronger noise in regional time-series than in global averages. The regional ToEs are also spatially heterogeneous, driven predominantly by the signal pattern akin to mesozooplankton. Additionally, our findings underscore that mitigation efforts (i.e., transitioning from SSP5-8.5 to SSP1-2.6 scenario) can potentially curtail emerging ocean surface signals by 30%.

Plain Language Summary Climate change will significantly impact global marine fish biomass, leading ecosystems into unprecedented states. The Time of Emergence (ToE) is when such a shift occurs. This study investigates the ToE of marine fish biomass using climate-to-fish simulations. Our results suggest that the emergence of global mean fish biomass occurs in the historical period (before 2020) and is controlled by small-size organisms (mesozooplankton) through food availability. We also show that the ToE strongly depends on organism size and varies regionally. Furthermore, we demonstrate that implementing mitigation policies significantly reduces the areas where marine ecosystems emerge, thereby limiting the potential negative impacts of climate change.

1. Introduction

Anthropogenic climate change is expected to significantly impact the abundance and spatial distribution of pelagic communities of high trophic level organisms (HTL) (Lefort et al., 2015; Lotze et al., 2019; Tittensor et al., 2021). These impacts on HTLs arise from a myriad of climate-related stressors encompassing changes in lower trophic level organisms (LTL, i.e. microzooplankton, mesozooplankton), temperature, oxygen concentration, pH and ocean currents (Bijma et al., 2013; Bopp et al., 2013). Yet, the foremost pivotal factors driving these changes remain changes in temperature and primary production (Heneghan et al., 2021; Pörtner & Peck, 2011). Ocean warming, in particular, is expected to accelerate metabolic rates and, thus, energy dissipation. In addition, temperature changes can affect the food consumption of organisms in different ways depending on the available food concentration (Guiet et al., 2016), resulting in a complex and diverse ecosystem response to temperature changes. These changes are generally anticipated to potentially reduce HTL biomass for a given level of primary production (Heneghan et al., 2019). Moreover, ocean temperature changes are anticipated to cause a global decline in primary production (Pörtner et al., 2022), notably through increased stratification, which reduces

nutrient concentrations in the euphotic zone. This will induce a global decrease in LTL organisms, the fundamental energy source fueling marine ecosystems (Chavez et al., 2011), and a marked reduction in fish biomass. Given the importance of marine resources for food security and the global economy, it is imperative to identify when and where these climate-induced impacts will exceed the natural variations of marine ecosystems.

The Time of Emergence (ToE), defined by Hawkins and Sutton (2012), represents when a climate change signal becomes distinguishable from the inherent natural variability. ToE is typically identified when the ratio of anthropogenic signal (S) to natural climate noise (N), expressed as SNR, permanently exceeds a predetermined threshold (as seen in studies such as Giorgi & Bi, 2009). Historically conceived to assess when local climates deviate from their historical norms, ToE analysis holds particular relevance for ecosystems with limited adaptive capacity (Beaumont et al., 2011; Deutsch et al., 2008). Applied initially to terrestrial areas (Diffenbaugh & Scherer, 2011; Giorgi & Bi, 2009), this concept has been extended to analyze changes in key environmental drivers of marine ecosystems, encompassing physical (Santana-Falcón & Séférian, 2022; Ying et al., 2022) and biogeochemical variables (Henson et al., 2017; Keller et al., 2014; Rodgers et al., 2015). Earth System Model projections consistently indicate early emergence of sea surface temperature (SST) signals and much later emergence in primary production (Henson et al., 2017; Keller et al., 2014; Rodgers et al., 2015; Schlunegger et al., 2020). However, the ToE concept has not yet been applied to pelagic ecosystem projections.

Marine Ecosystem Models (MEMs) have been pivotal in projecting and understanding the impacts of climate change on marine ecosystems, notably through initiatives such as the Fisheries and Marine Ecosystem Model Intercomparison Project (FishMIP, Lotze et al., 2019; Tittensor et al., 2018, 2021). On average, these projections indicate a reduction in global fish biomass at the end of the century of around 15%–20% in a high emissions scenario (SSP5-8.5) and of around 5%–7% in a low emissions scenario (SSP1-2.6) (Lotze et al., 2019; Tittensor et al., 2021). In addition, these studies highlight a spatial heterogeneity in the fish biomass response to climate change, hinting at potential increases in the Arctic and Southern Oceans while predicting decline elsewhere.

The primary objective of this study is to implement the ToE concept within projections generated by a global-scale marine ecosystem model, examining and contrasting these ToE with the pivotal environmental variables driving this model. Using the mechanistic Marine Ecosystem Model APECOSM forced by ensemble simulations from the IPSL-CM6A-LR Earth System Model for two contrasted emission scenarios (SSP5-8.5 and SSP1-2.6), we will first show that, when considering the global average, the ToE is very early for the epipelagic (1950) and later for the migratory (2036) and mesopelagic (2017) fish biomass, with a strong dependency to the size class considered. Next, we show that the ToE at the regional scale is considerably later than the globally averaged one, with a strong dependency on the region and community considered. The paper is structured as follows. Section 2 describes the ecosystem and climate models, the simulation protocol and the methodology used to calculate the ToEs. Section 3 compares the ToEs estimated for the main ecosystem drivers, namely ocean temperature and mesozooplankton concentration, with those estimated for fish biomass. Finally, Section 4 discusses this work's limitations and perspectives and synthesizes our results.

2. Data and Method

2.1. Marine Ecosystem Model

This study uses the Apex Predators ECOSystem Model (APECOSM, Maury et al., 2007; Maury, 2010) to simulate changes in marine fish biomass in the global ocean. APECOSM is an Eulerian ecosystem model that mechanistically represents the three-dimensional dynamics of size-structured pelagic populations and communities. It integrates individual, population and community levels and includes the effects of life-history diversity with a trait-based approach (Maury & Poggiale, 2013). Energy uptake and use for individual growth, development, reproduction, somatic and maturity maintenance are modeled according to the Dynamic Energy Budget (DEB) theory (Koojman, 2010), with metabolic rates dependent on food and temperature.

APECOSM also includes important ecological processes such as opportunistic size-structured trophic interactions and competition for food, predatory, disease, aging and starvation mortality, key physiological aspects such as vision and respiration, as well as essential processes such as three-dimensional passive transport by marine currents and active habitat-based movements (Faugeras & Maury, 2005), schooling and swarming (see Maury, 2017; Maury & Poggiale, 2013; Maury et al., 2007).

Table 1
Summary of the Numerical Simulations Used in This Study

Simulation	Initial conditions	Simulation period
piControl-spinup	Uniform biomass distribution	1750–1850
piControl	*piControl-spinup*	1850–2029
hist-r1	*piControl* (1909-12-31)	1850–2014
hist-r2	*piControl* (1869-12-31)	1850–2014
hist-r3	*piControl* (1929-12-31)	1850–2014
hist-r4	*piControl* (1949-12-31)	1850–2014
hist-r6	*piControl* (2029-12-31)	1850–2014
hist-r14	*piControl* (1969-12-31)	1850–2014
ssp-r1	*hist-r1*	2015–2100
ssp-r2	*hist-r2*	2015–2100
ssp-r3	*hist-r3*	2015–2100
ssp-r4	*hist-r4*	2015–2100
ssp-r6	*hist-r6*	2015–2100
ssp-r14	*hist-r14*	2015–2100

Note. Simulation names (first column) are shown in italic. The middle column indicates the initial conditions used. For the historical simulations, the *piControl* year from which the initial conditions are extracted is indicated. The last column indicates the simulation period. *Ssp* indicates the climate change simulations, considering either the SSP1-2.6 or SSP5-8.5 scenarios.

In this study, we used the same APECOSM configuration as in Barrier et al. (2023), in which the model was used to analyze the ENSO-related variability of the epipelagic fish biomass in the tropical Pacific Ocean. Three generic communities are simulated.

- The epipelagic community includes the organisms inhabiting surface waters day and night. Its vertical distribution is affected by light and visible food during the day, as well as by temperature and oxygen. Additionally, its functional response to prey is influenced by light and temperature.
- The migratory mesopelagic community includes organisms that feed in the surface layer at night and move to deeper waters during the day. Its vertical distribution is determined by light during both day and night and visible food during the night.
- The resident mesopelagic community includes organisms that remain at depth during both day and night. Its vertical distribution is influenced by light and visible food during the day.

The Supporting Information S1 provide a more detailed description of the APECOSM model and of the 3 community configuration used in this study, following the description of Barrier et al. (2023).

2.2. Climate Model

In this study, APECOSM is forced by 3D physical and biogeochemical outputs of the IPSL-CM6A-LR Earth System Model (ESM) (Boucher et al., 2020). This ESM has recently been used by the Fisheries and Marine Ecosystem Model Intercomparison Project (FishMIP) to assess the impacts of climate change on marine ecosystems (Tittensor et al., 2021). The Supporting Information S1 provide the list of variables needed by APECOSM.

2.3. APECOSM Simulations Protocol

This section describes the APECOSM simulation protocol. For simplicity, the acronyms of the APECOSM simulations are identical to those of the climate simulations used as forcing.

First, a 100-year spin-up simulation (*piControl-spinup*) was performed, starting with a uniform biomass distribution for each community and size class. The end of this spin-up simulation is then used to restart a pre-industrial climate simulation (*piControl*). In these two simulations, CO_2 concentrations are fixed at pre-industrial levels.

Next, six members of the historical scenario (*historical*), constrained by observed greenhouse gas emissions, have been run from 1850 to 2014. The initial conditions of each member were sampled every 20 or 40 years from the *piControl* simulation (Boucher et al., 2020). Finally, the end of the six historical simulations has been used to initialize the climate change simulations. Two scenarios were considered, the SSP5-8.5 and SSP1-2.6 "Shared Socioeconomic Pathways" scenarios, which represent the upper and lower ends of the CMIP6 future radiative forcing, with projected warming in 2100 reaching 4°C for the SSP5-8.5 scenario and weaker than 2°C for the SSP1-2.6 scenario (O'Neill et al., 2016).

The details of the simulation protocol are provided in Table 1 and a schematic is provided in Figure S1 of Supporting Information S1.

2.4. Time of Emergence

As discussed in the introduction, ToE typically marks when the ratio of anthropogenic signal (S) to natural climate noise (N), expressed as SNR, permanently exceeds a predefined threshold (Giorgi & Bi, 2009). In this section, we illustrate the methodology used to calculate the signal S, the noise N and the ToE using time series of global mean epipelagic fish biomass as an example.

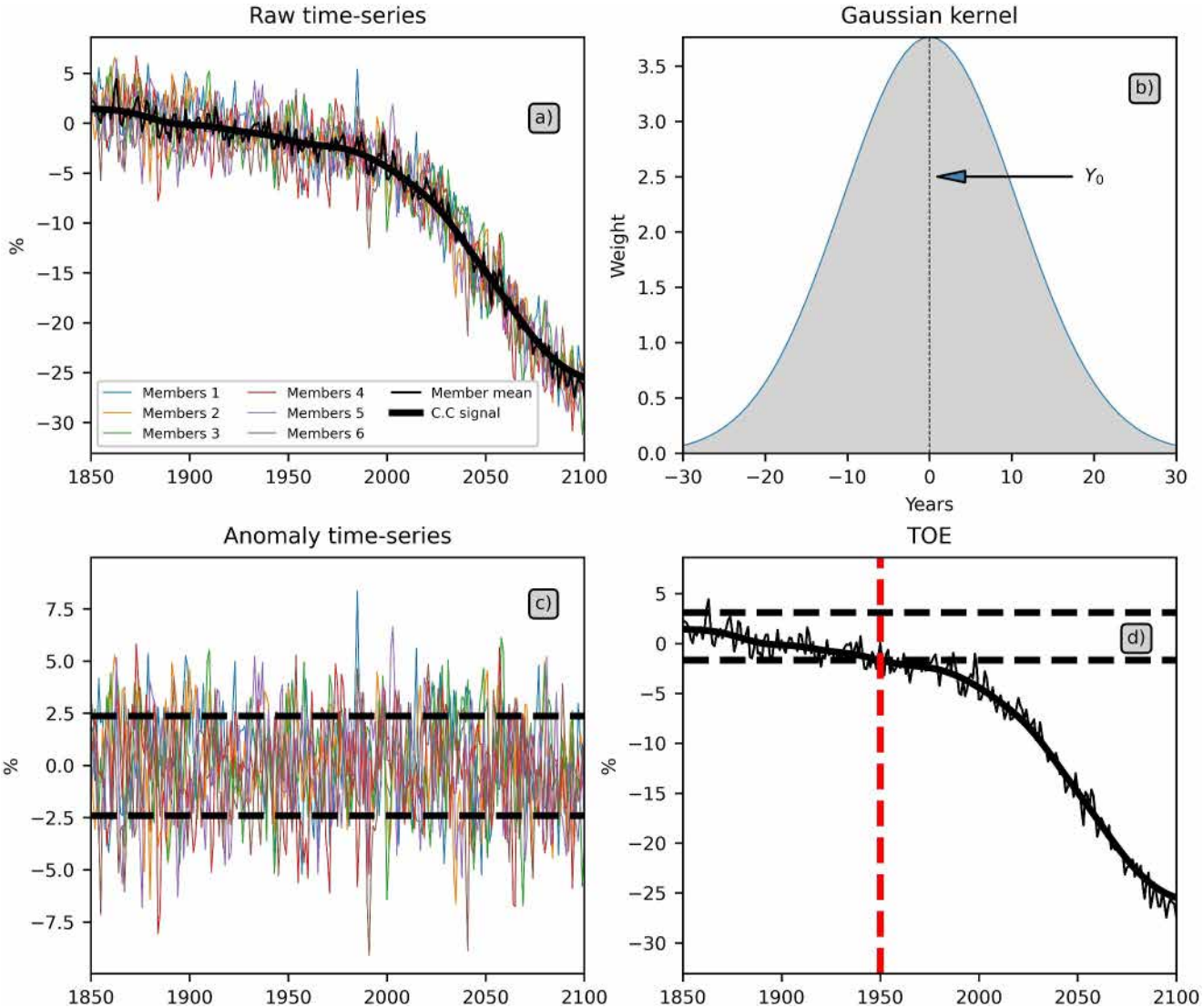

Figure 1. Overview of steps for calculating the time of emergence. Displayed is the time series for global mean epipelagic fish biomass. (a) Single-member time series (colored lines), multi-member mean (thin black line) and climate change signal (thick black line). (b) Illustration of the Gaussian kernel that was used to smooth the multi-member mean. (c) Computed noise was obtained by subtracting the climate change signal from the original time series. These anomalies represent the range of natural variability (dashed lines). (d) Calculation of the time of emergence (dashed red line) as the moment when the climate change signal is permanently outside the range of natural variability.

The methodology employed in Hawkins & Sutton (2012) for signal estimation, which assumes a proportional scaling between local changes and global variations, cannot be applied in our context. While this assumption holds at first order for SST, it does not hold for biogeochemical and biological variables, whose climate change signal shows substantial spatial and temporal heterogeneity (Lotze et al., 2019; Tittensor et al., 2021). Instead, the climate change signal in our approach is derived by averaging the historical and scenario time series over the six members, as shown in Figure 1a (thin black curve). Since these members share identical external forcings and differ only in their initial state, the multi-member average is a good first approximation of the climate change signal. However, residual noise persists due to the limited number of available members. To remove this residual noise, a Gaussian filter with a standard deviation of 15 years is applied to smooth the multi-member mean (Figure 1b). The resulting smoothed time series (thick black curve in Figure 1a) is regarded as the climate change signal S.

Natural variability is then estimated by removing this climate change signal from each member time series. The resulting time series (Figure 1c) represents the anomalies in fish biomass solely due to high-frequency climate and

ecosystem variability. The noise N is then estimated by calculating the standard deviation of the anomalies over the time and member dimensions (black dashed curve in Figure 1c).

Finally, we define ToE as the year when the climate change signal permanently exceeds the envelope of natural variability (black dashed curve in Figure 1d), which we define as the historical multi-member mean computed between 1850 and 1900 plus or minus the standard deviation of the anomalies (N, Figure 1d). To avoid potential artifacts due to truncation of the Gaussian smoothing kernel used to extract the signal, we consider that there is no emergence if the estimated ToE is later than 2085.

ToEs are calculated globally and at each grid cell for temperature at the surface and averaged between 500 and 1,000 m, surface mesozooplankton concentrations, and for the vertically integrated fish biomass density of each community and each size class. In addition, total fish biomass (i.e., biomass integrated over the entire size range) is also evaluated for each community.

3. Results

This section first discusses the ToE for global mean temperature at the surface and between 500 and 1,000 m, surface mesozooplankton concentrations and global mean total biomass for each fish community and each size-class. This section allows illustrating the ToE concept on single time series and aligns with many FishMIP studies that analyze globally averaged biomass time series (Heneghan et al., 2021; Lotze et al., 2019; Tittensor et al., 2021). It helps identify when global fish biomass changes have been or will be detected. Furthermore, although the analysis of ToE by size class is crucial, incorporating spatial dimensions renders the analysis more intricate. The spatial aggregation of biomass offers a means of simplifying this analysis.

3.1. Global Mean ToE

3.1.1. Environmental Drivers and Total Fish Biomass

Figure 2 shows the global mean anomalies of temperature at the surface (SST) and averaged between 500 and 1,000 m, surface mesozooplankton concentrations and fish biomass density (integrated between 0 and 1,000 m) of each community relative to the 1850–1900 period. Global SST starts rising by 1900, with accelerated warming post-2000 under the SSP5-8.5 scenario (red curve), exceeding 3.5° by the end of the 21st century (Figure 2a). Under SSP1-2.6, the warming reaches a plateau from the middle of the century (around 1.5°). Due to minimal noise attributable to the global averaging, global SST emerges very early (1915) in both scenarios. The warming between 500 and 1,000 m (Figure 2b) is weaker than the SST's and starts later, resulting in a delayed emergence (around 1945).

Global surface mesozooplankton anomalies exhibit a decrease in both scenarios (Figure 2c), opposing the warming of temperature anomalies. Under SSP5-8.5, they decline sharply at the turn of the 21st century, continuing linearly to −15% by the century's end. Under SSP1-2.6, the decline moderates, plateauing at −5% by 2050. The weaker signal-to-noise ratio for mesozooplankton results in a later emergence (2001) than SST (1915).

Epipelagic fish biomass evolution (Figure 2d) is similar to mesozooplankton's, suggesting a bottom-up control. However, by the century's end, the relative decline in epipelagic biomass surpasses that of mesozooplankton for both scenarios. This more significant decline is likely linked to trophic amplification from warmer temperatures (de Luzinais et al., 2023), leading to an early emergence of global mean epipelagic biomass (1950).

Mesopelagic biomass evolution (Figure 2f) closely matches that of epipelagic biomass in both timing and amplitude, but also that of mesozooplankton and detritus concentrations (not shown), which are their primary food source, again suggesting a bottom-up control mechanism. Despite similar relative noise levels (2%), mesopelagic biomass declines more slowly than epipelagic biomass, resulting in later emergence (2017). This slower decrease is likely due to weaker early stage warming in the mesopelagic zone than in the epipelagic zone (Figures 2a and 2b). Initially, the warming affects the surface layers and gradually penetrates deeper, causing a weaker trophic amplification early on. Over time, as surface warming signals penetrate deeper, trophic amplification increasingly impacts the mesopelagic community.

Compared to the other communities, the climate change signal of the migratory community (Figure 2e) is weaker by 2100 in both scenarios. This weaker signal leads to a late emergence under SSP5-8.5 (2036) and no emergence under SSP1-2.6, as the climate change signal never exceeds the range of natural variability. This reduced signal

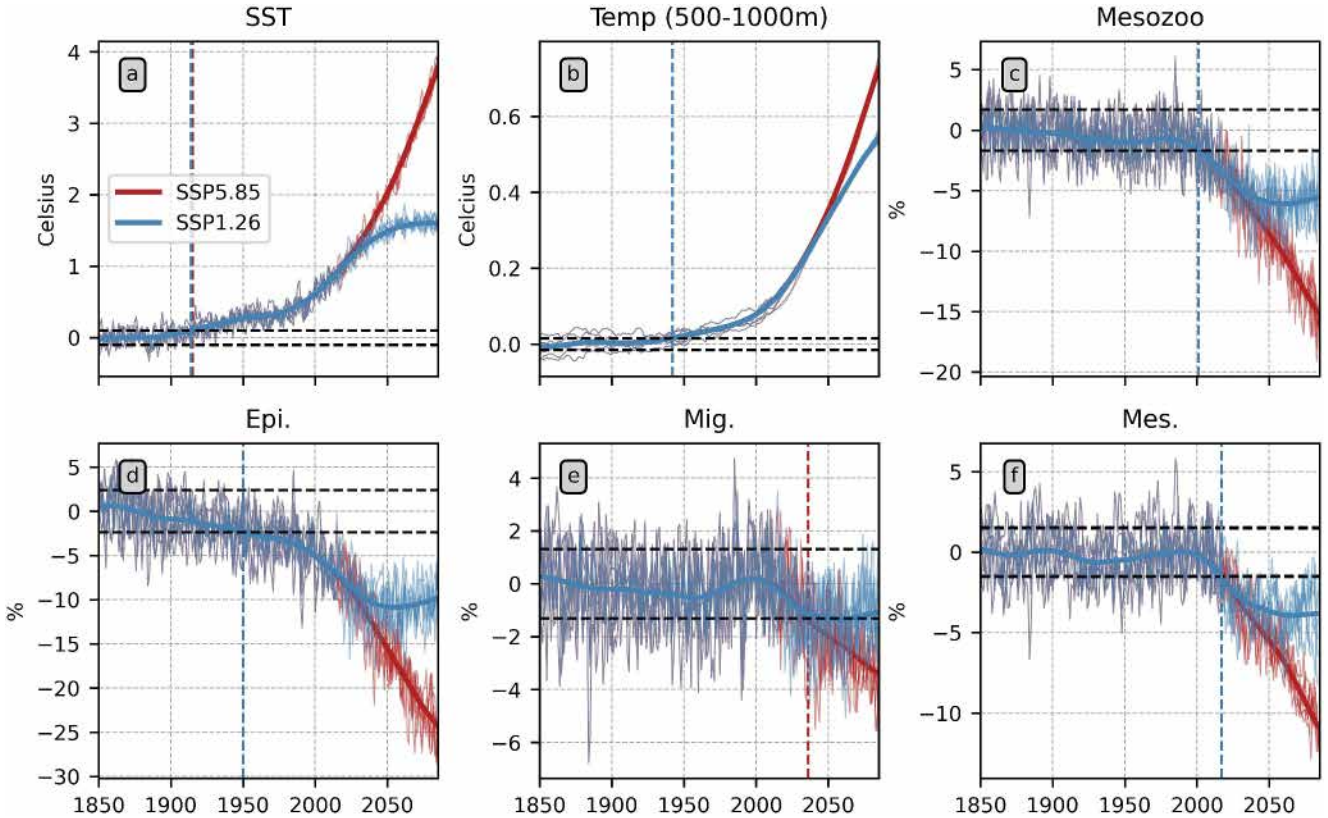

Figure 2. Global mean anomalies of surface temperature (a), temperature averaged between 500 and 1,000 m (b), relative surface mesozooplankton concentrations (c), and global mean fish biomass for the epipelagic, migratory, and mesopelagic communities (d, e, f). The thin lines represent the individual members, and the thick lines represent the climate change signal.

for the migratory community is probably the result of two opposing effects. Because they live at depth during the day, in waters where the temperature is cooler and warms less rapidly than at the surface, their metabolic processes use less energy and this energy demand increases less rapidly with climate change than for epipelagic fish living at the surface. Furthermore, despite experiencing a comparable reduction in epipelagic prey availability as the epipelagic community, the significant migratory mesopelagic component of their prey (intra-community predation) declines less rapidly. The dissipative processes in the resident mesopelagic community, on the other hand, are increasing even more slowly, and the decline in the amount of their preys, which includes a migratory mesopelagic component and a detrital component from the epipelagic zone, is decreasing at a rate intermediate between these two components.

3.1.2. ToE Sensitivity to the Fish Size Class

As discussed, for example, in Barrier et al. (2023), the response of marine fish biomass to changes in environmental drivers is size-dependent. Consequently, the natural variability N, the climate change signal S and, hence, the ToE of fish biomass are expected to vary with size. In the following, we examine the ToE sensitivity to the organism size class for each community and the primary factor governing this sensitivity, whether it is noise or signal. For the sake of clarity, the focus is on the SSP5-8.5 scenario. However, the same analysis has been performed on SSP1-2.6 and is available in Supporting Information S1.

The upper panels in Figure 3 show the ToE as a function of size for each community. In contrast, lower panels illustrate the signal-to-noise ratio (SNR), the relative signal (S) and the relative noise (N). For the epipelagic community, the ToE is early (1950) and stable for size classes smaller than 1 cm (Figure 3a). Then it increases from 1950 to 1990 for sizes ranging from 1 to 15 cm. This increase can be directly related to the rise in the noise within this size range (Figure 3j), resulting in a weaker SNR (Figure 3d) and therefore a delayed emergence. For sizes exceeding 15 cm, the ToE experiences a steep decline, with the largest organisms (1 m) reaching an

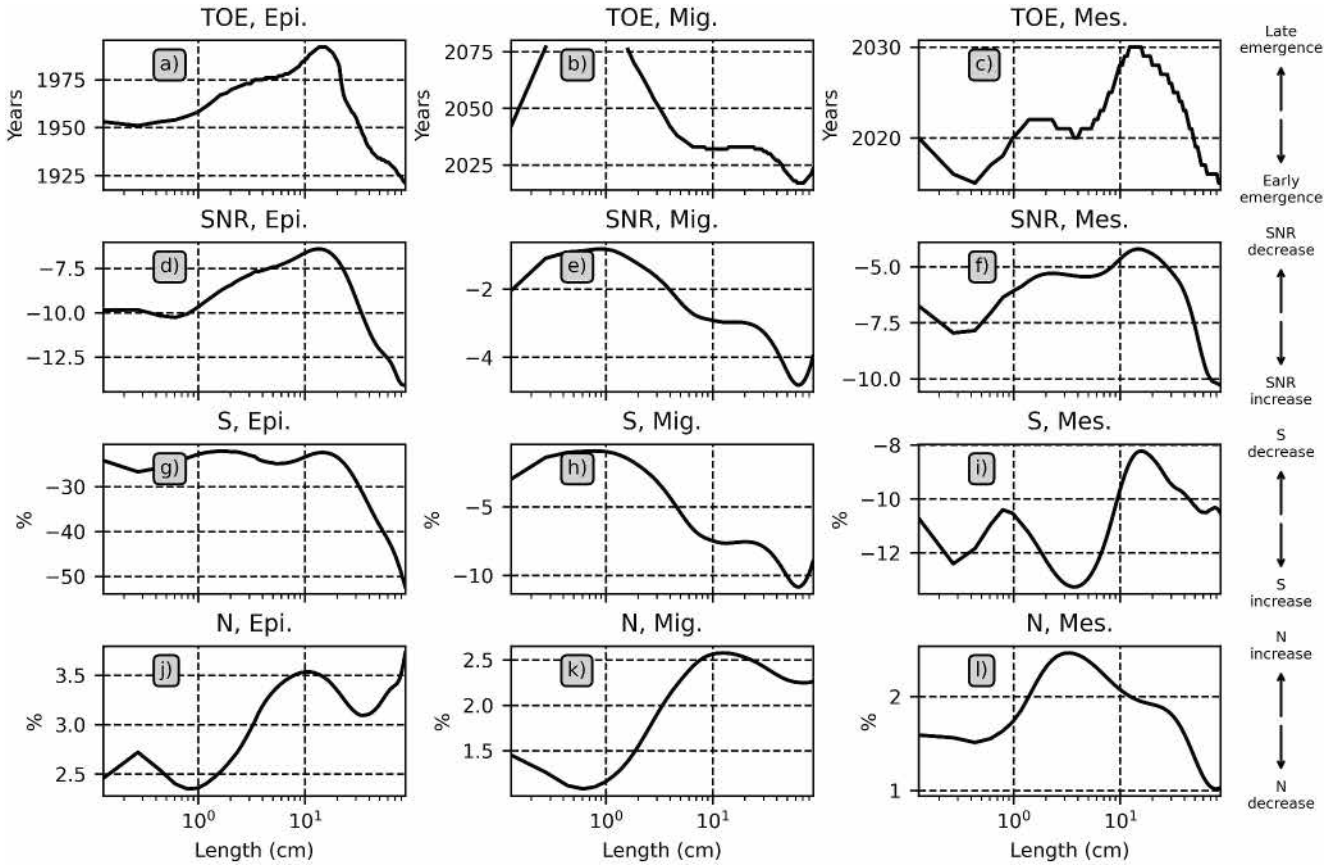

Figure 3. Time of emergence (a–c), signal-to-noise (d–f) ratio, relative signal (g–i) and relative noise (j–l) for epipelagic (left), migratory (middle) and resident (right) mesopelagic communities in the SSP5-8.5 scenario. The *y*-axis has been ordered to facilitate the comparison of the signal-to-noise ratio with its components. Signal *S* is calculated as the multi-member mean difference between the SSP5-8.5 biomass averaged over the 2070–2100 period and the historical biomass averaged between 1850 and 1900. Noise *N* is computed as indicated in Section 2.4.

emergence date of 1920. This decline can predominantly be attributed to a signal increase within this size range (Figure 3g).

The signal of the migratory community does not emerge for size classes between 0.4 and 1.4 cm (Figure 3b). This is due to a weak signal (Figure 3h), leading to a negligible SNR (Figure 3e) around these size classes. For sizes larger than 1.4 cm, the ToE decreases with size, ranging from 2075 for small sizes to 2025 for large ones. This early emergence for larger organisms is due to a strong signal (−4%, Figure 3h).

The changes in ToE with sizes are less clear for the resident mesopelagic community (Figure 3c) than for the other two communities. From 0 to 1 cm, the changes in ToE are driven by changes in signal (Figure 3i). From 1 to 5 cm, the ToE is stable (around 2020), mainly due to opposite changes in both signal and noise (Figure 3l). Then, the ToE increases, reaching 2030 for 10 cm, due to a substantial reduction in the signal *S*. Finally, the ToE drops for larger sizes (2015 for 90 cm) due to the combined effects of increased signal and reduced noise.

3.2. Regional ToE

This subsection analyses the spatial patterns of the ToE for SST, mesozooplankton and fish biomass for each community. For the sake of simplicity, only the results for the SSP5-8.5 scenario will be discussed. However, the same analysis for SSP1-2.6 can be found in Supporting Information S1.

3.2.1. Comparison With Global Mean ToE

The previous subsection demonstrates that, when globally averaged, fish biomass signals emerge early, mainly during the historical period. This result is likely related to a significant reduction in noise through spatial

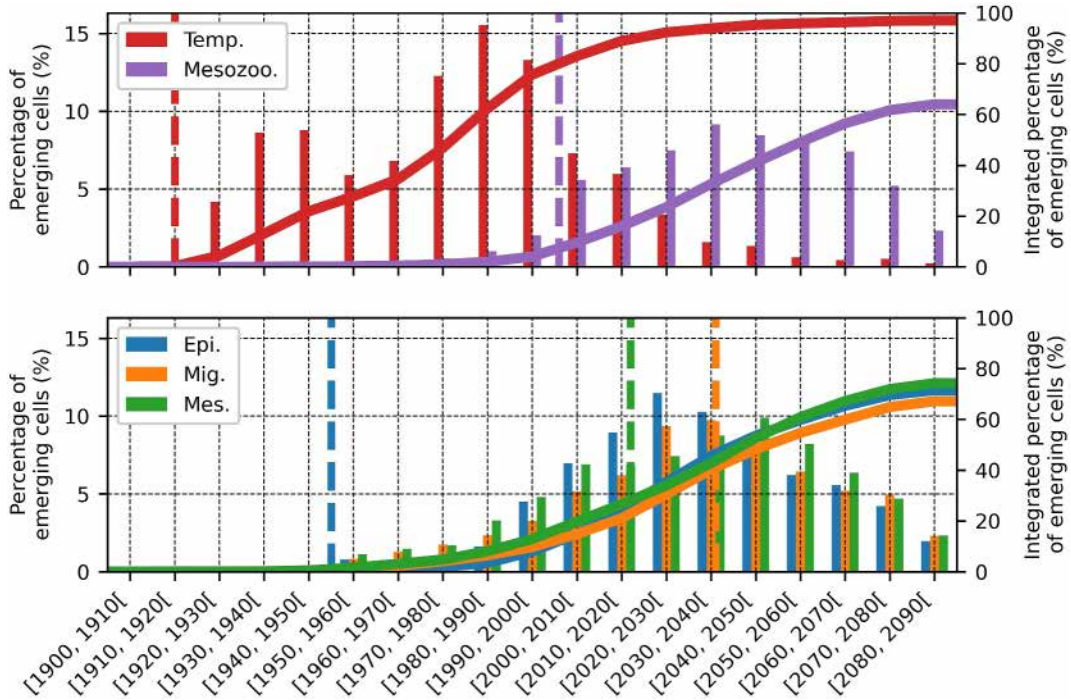

Figure 4. Percentage of the ocean surface where a signal has emerged in the SSP5-8.5 scenario during a given decade (*x*-axis) for SST (red bars) mesozooplankton concentration at the surface (purple bars), biomass of the epipelagic fish community (blue), migratory mesopelagic fish community (orange), resident mesopelagic fish community (green). The continuous lines show the corresponding cumulative percentages. The dashed vertical lines indicate the ToE of the global mean time series.

averaging, leading to an increase in SNR. In this subsection, the ToE calculated at each grid point (1° to 1/3° in the equatorial band) is compared to the ToE of the global mean time series.

Figure 4 shows the percentage of the ocean surface where a signal emerges during a given decade (vertical bars) in the SSP5-8.5 scenario, alongside the cumulative surface where a signal has emerged over time (continuous line). SSTs exhibit early regional emergence, starting between 1920 and 1930 and peaking between 1970 and 1990. Regarding cumulative percentage, SST signals have emerged over about 90% of the ocean surface by 2020, reaching 97% by the end of the century. In contrast, regional mesozooplankton biomass emerged around 1970 and peaked in 2030. By 2020, mesozooplankton has emerged over only 23% of the ocean surface, gradually increasing to 64% by the end of the century. This corresponds to a difference of approximately 50 years between the regional ToE of mesozooplankton and the regional ToE of SST.

The timing of regional emergence for total fish biomass is comparable for all three communities, with the mesopelagic and migratory communities emerging slightly before the epipelagic community. Consequently, the percentages of the ocean surface showing emergence are qualitatively similar between the three communities, ranging from 30% to 34% by 2020 and 67%–74% by 2100. The timing of emergence for regional fish biomass is similar to that of mesozooplankton (purple curve) but about a decade earlier, especially for epipelagic organisms, confirming both the bottom-up influence of lower trophic levels on higher trophic levels and the trophic amplification phenomenon already discussed for global scale (Figure 2).

For all variables except one, the peaks of regional emergence occur later than the emergence of the global mean time series. For example, the peak of regional SST emergence occurs 60 years later than the emergence of the global mean SST. In comparison, the lag is about 30 years for the mesozooplankton and mesopelagic fish communities and 75 years for the epipelagic community (dashed lines in Figure 4). The exception is the migratory fish community, for which the peak of regional emergence occurs during the same decade (2030–2035) as the emergence of global mean biomass.

Figure 5 compares the 10^{th}, 25^{th}, 50^{th} (median), 75^{th} and 90^{th} percentiles of the local noise N (upper panels), signal S (middle panels) and ToE (lower panels) distributions with the values obtained from the global mean time series

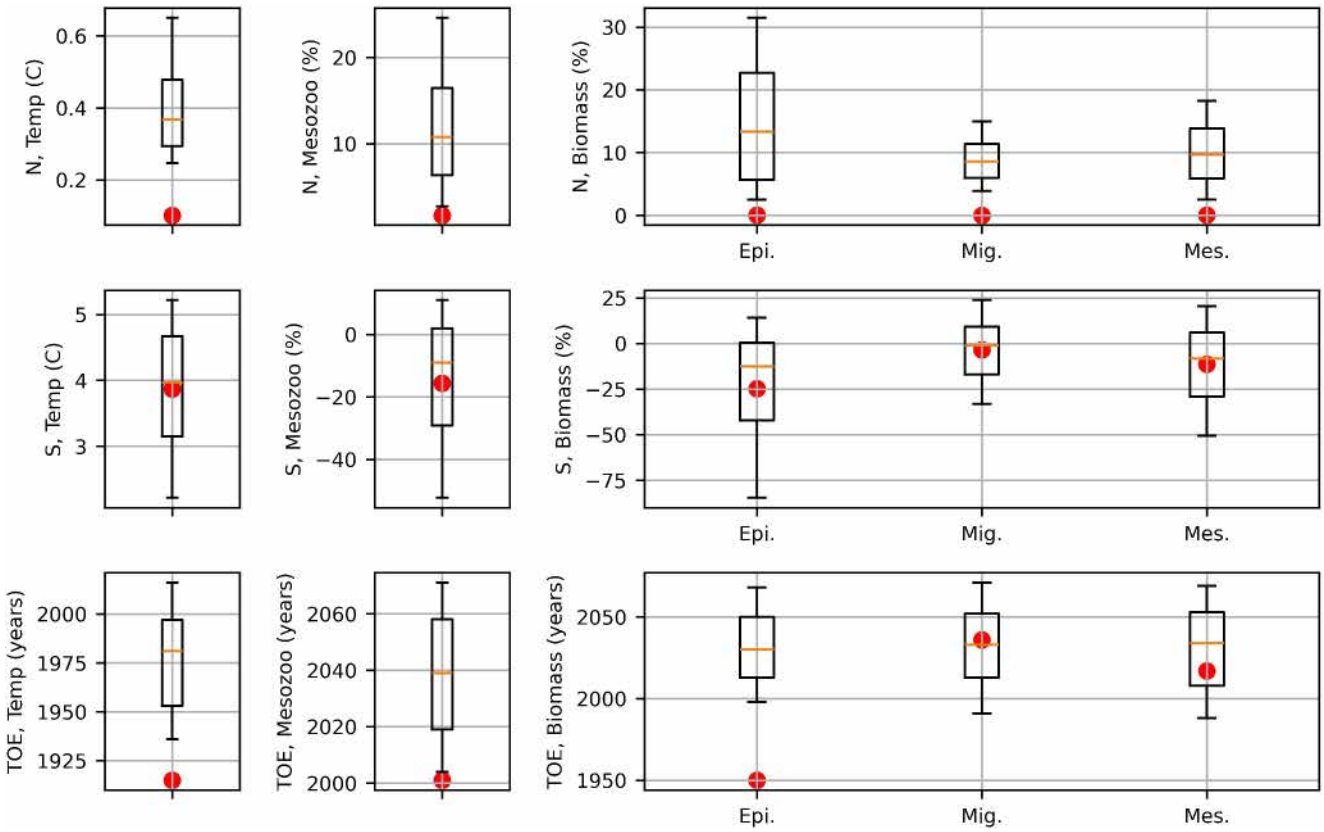

Figure 5. Whisker plot showing the 10^{th}, 25^{th}, 50^{th}, 75^{th} and 90^{th} percentiles of spatial noise *N*, signal *S* and ToE for sea surface temperature, surface mesozooplankton and fish biomass in the SSP5-8.5 scenario. Red dots indicate the values obtained from the global time series. Mesozooplankton and fish biomass noise and signal are represented in anomalies relative to the historical (1850–1950) mean value.

(red dots). In all cases, the noise values for global averages are smaller than the 10^{th} percentile of the local noise. Conversely, the global mean signal aligns more closely to the signal calculated locally, falling between the 25^{th} and 75^{th} percentiles for all variables. Nevertheless, the global mean ToE for fish biomass falls between the 25^{th} and 75^{th} percentiles of the regional ToE, except for the epipelagic community, for which the global mean ToE is 50 years earlier than the 10^{th} percentile.

3.2.2. Spatial Patterns

In the following, the spatial patterns of ToE for SST, surface mesozooplankton and total fish biomass per community are analyzed.

3.2.2.1. Sea Surface Temperature

Figure 6a shows the ToE map for SST. As expected from Figure 4, most oceanic regions emerge early. In particular, the earliest emergence occurs in the tropical Indian Ocean, the tropical Atlantic and the Western Pacific. However, several areas exhibit a late emergence, such as the eastern equatorial Pacific, which manifests emergence around 2010, along with mid-latitude regions and Antarctica. These patterns are consistent with findings from previous studies derived from other ESMs (see, for instance, Figure 4 of Schlunegger et al. (2020)).

Figure 6b shows the SNR map for SST, which is closely related to ToE. Here, the noise (Figure 6c) is defined as the standard deviation of the anomalies relative to the climate change signal (see Section 2.4). The signal (Figure 6d) is the difference between the SSP5-8.5 multi-member mean SST averaged between 2070 and 2100 and the historical multi-member SST averaged between 1850 and 1900. The SNR pattern mirrors the ToE map, indicating an early emergence in regions with a large SNR ratio and a late emergence in areas with a smaller ratio. The SST signal (Figure 6d) shows much less spatial variation than the noise (Figure 6c), and the SNR is

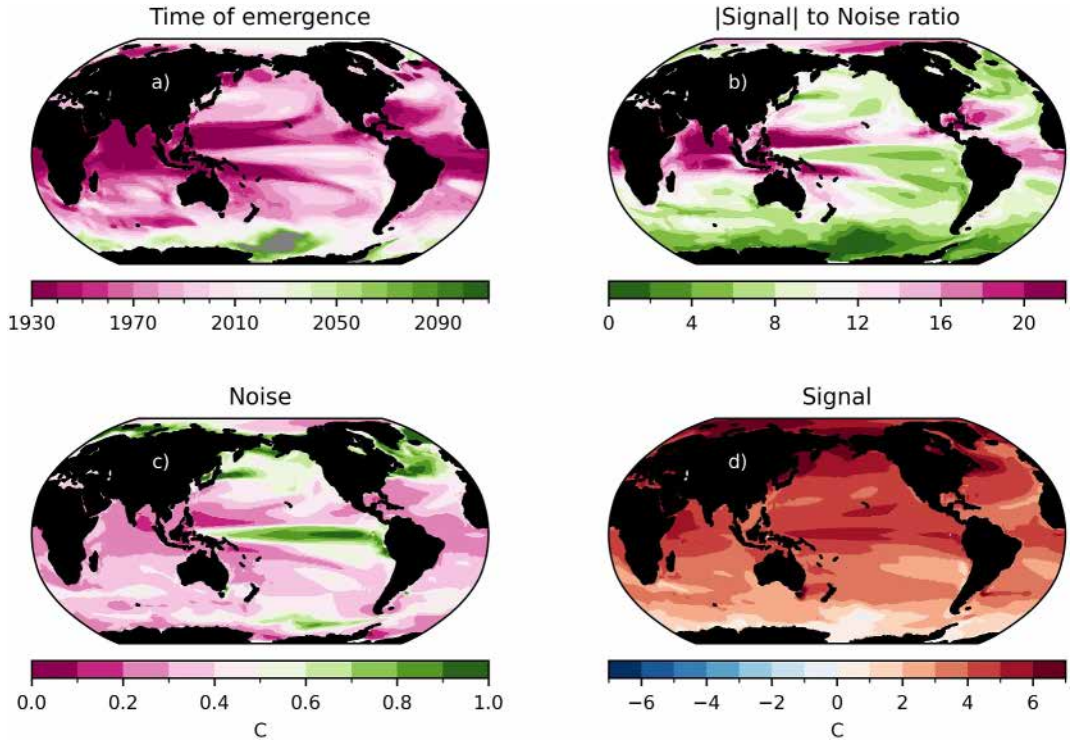

Figure 6. Maps of ToE (a), SNR (b), noise *N* (c), and signal *S* (d) for SST in the SSP5-8.5 scenario. Noise is calculated as the standard deviation of the anomalies relative to the climate change signal (see Section 2.4). The signal is calculated as the multi-member mean difference between the SSP5-8.5 SST averaged over the 2070–2100 period and the historical SST averaged between 1850 and 1900. In (a), gray shadings indicate areas that have not emerged.

predominantly influenced by the noise, with a spatial correlation between the SNR and the inverse of the noise reaching 0.71. In particular, the considerable noise and, hence, the late emergence of SST in the tropical Pacific are related to the strong ENSO variability (Diaz et al., 2001). Similarly, in the North Pacific and the Atlantic oceans, delayed emergence arises from the considerable noise induced by the Pacific North American pattern and the North Atlantic Oscillation (Hurrell & Deser, 2009), respectively. The correlation of SNR with the signal is 0.47. In particular, the weak SNR and, hence, the late emergence of SST in the Southern Ocean is due to a weaker signal.

3.2.2.2. Surface Mesozooplankton

As expected from Figure 4, the ToE map for mesozooplankton (Figure 7a) shows broad regions where the signal has not emerged by the end of the century. Signals have emerged in most tropical oceans, with early emergence occurring in the equatorial Atlantic, western Pacific and western Indian Ocean. On the contrary, ToE patterns are more patchy and less homogeneous at mid and high latitudes, with early emergence in the subtropical Pacific gyres (2010) and no emergence on their flanks. Compared to the SST, the mesozooplankton signal (Figure 7d) displays huge spatial variations, from a substantial decrease in the tropics, especially in the equatorial Atlantic and western Pacific, to a significant increase in the subtropical Pacific gyres. These regions with a prominent mesozooplankton response generally correspond to those with early emergence. In contrast to SST, the signal-to-noise ratio (Figure 7b) and hence the ToE for mesozooplankton is predominantly driven by the signal (spatial correlation of 0.59) rather than the noise (spatial correlation with the inverse of the noise of −0.02). This is particularly true in regions with the highest signal-to-noise ratio (pink areas in Figure 7b), which are associated with strong signals (either positive or negative). These regions are also the earliest to emerge (before 2010).

3.2.2.3. Fish Biomass

The SNR, and consequently the associated ToE, predominantly mirror the signal within the three communities, as illustrated in Figure 8. Areas exhibiting early emergence coincide with those displaying stronger positive or

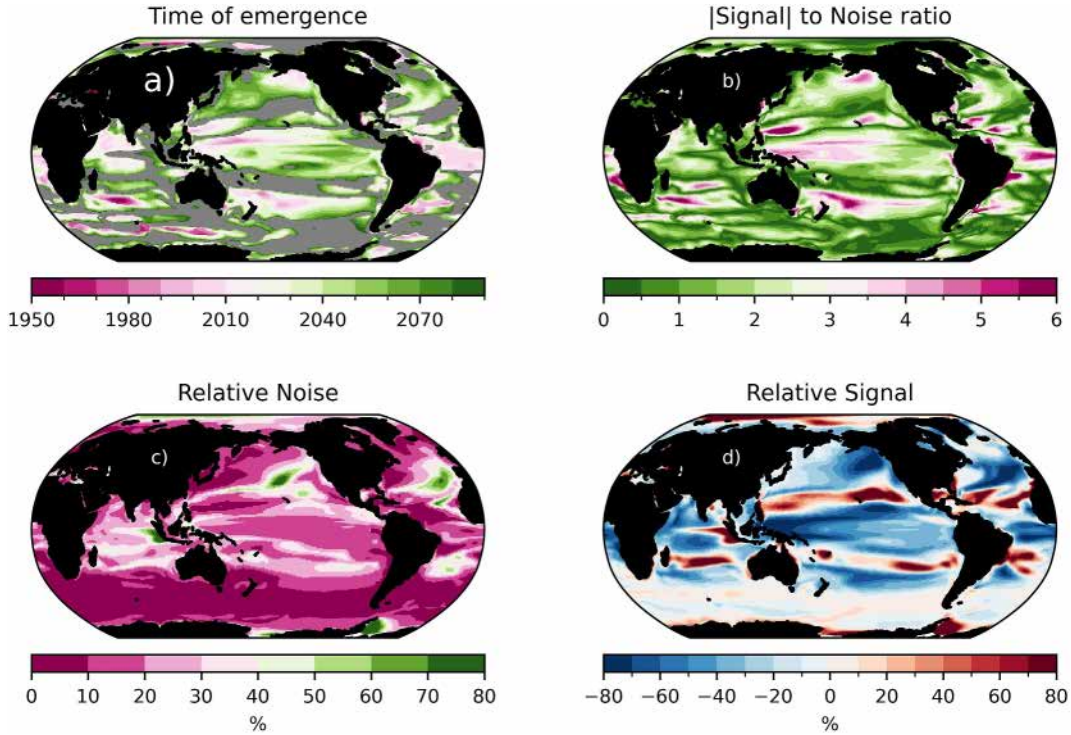

Figure 7. Time of emergence (a), signal-to-noise ratio (b), noise *N* (c) and signal *S* (d) for sea surface mesozooplankton concentration in the SSP5-8.5 scenario. The noise is given as the standard deviation of the anomalies relative to the climate change signal (see Section 2.4). The signal is provided as the multi-member mean difference between the SSP5-8.5 mesozooplankton averaged over the 2070–2100 period and the historical mesozooplankton averaged between 1850 and 1900. The latter is also used to normalize the noise and signal, which are presented as percentages. In (a), gray shading indicates areas that have not emerged.

negative signals. This visual assessment finds further support in the pattern correlation between the SNR and the relative signal, which reaches 0.64, 0.66 and 0.63 for the epipelagic, migratory and mesopelagic communities, respectively. Conversely, the correlation with the inverse of the relative noise is much lower (0.03, −0.11 and 0.1, respectively).

Although the three communities display a similar emergence timeline (Figure 4), the spatial patterns of their ToE show striking disparities, as illustrated in Figures 8a–8c. The epipelagic fish biomass emerges before 2020 in regions such as the tropical Pacific and Atlantic on both sides of the equator, the northern and southern Pacific and Atlantic Oceans, and the southeast of Madagascar (Figure 8a). These regions of early emergence align with the early emergence of mesozooplankton biomass (Figure 7a), which corresponds to a pronounced decline in mesozooplankton concentration (Figure 7d) and epipelagic fish biomass (Figure 8d). The projected signal patterns for the epipelagic community resemble those for mesozooplankton (pattern correlation of 0.54), indicating that changes in mesozooplankton concentration are the predominant drivers of projected changes in epipelagic fish biomass, as already inferred from global mean time series (Figure 2). This influence is more substantial than that of temperature, which exhibits a much earlier emergence and distinctly different patterns (Figure 6d, pattern correlation of −0.25). Although not structuring the ToE spatial patterns for the epipelagic community, warmer temperatures likely induce early emergence (median value around 2025, Figure 5), presumably through trophic amplification (de Luzinais et al., 2023).

There is a notable similarity between the ToE (Figures 8b and 8c) and signal patterns (Figures 8e and 8f) observed in migratory and mesopelagic communities, with a pattern correlation of around 0.61 between their two signal patterns, despite smaller values for the migratory community than for the mesopelagic community. The most striking feature is the very early emergence, which occurs around 1950 in the central Pacific at approximately 15°N. This area of early emergence coincides with a strong positive mesozooplankton concentration signal in the gyres (Figure 7d), which in turn leads to a marked increase in the mesopelagic and migratory fish biomass

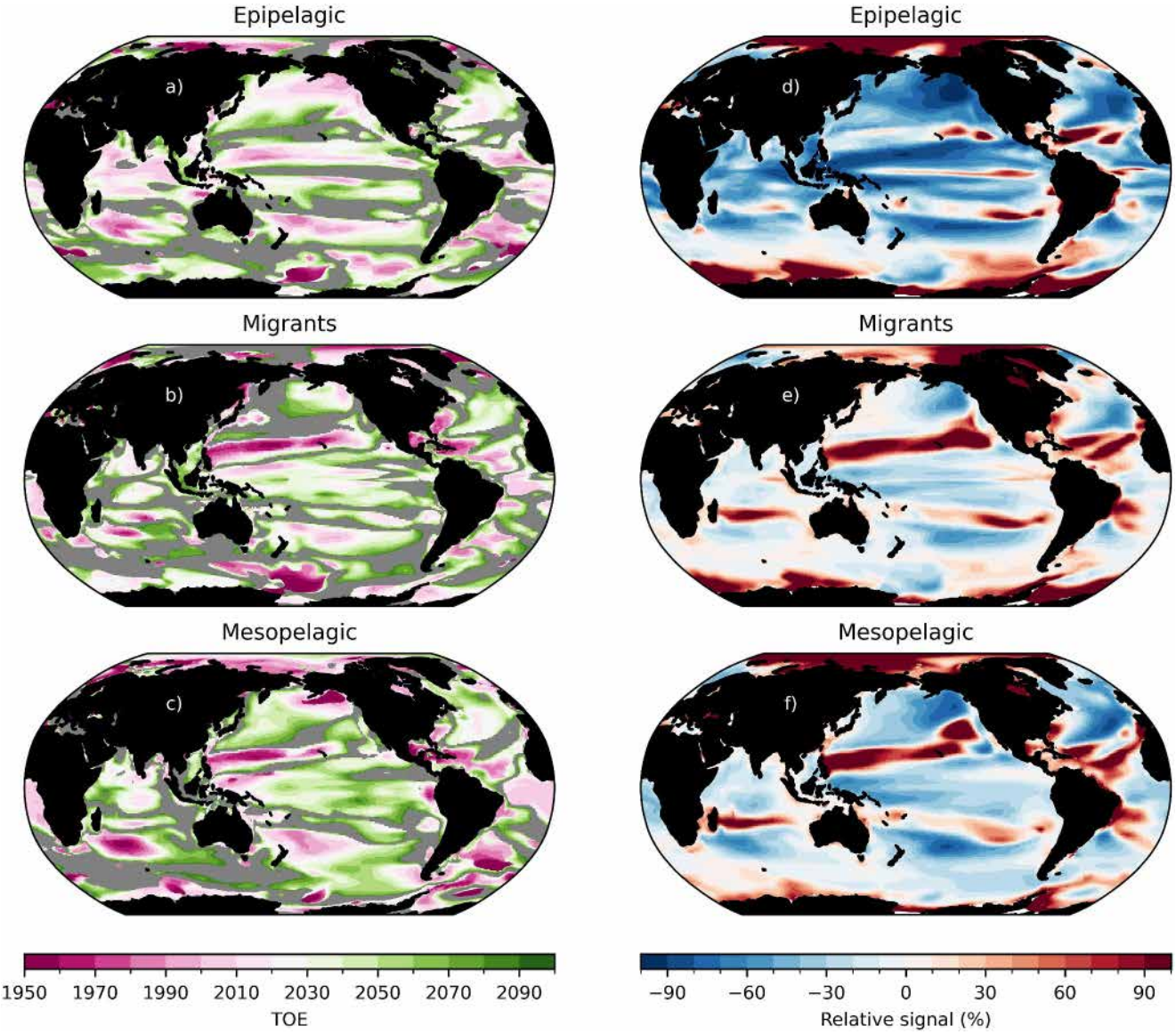

Figure 8. (a, b, c) ToE maps of fish biomass in the SSP5-8.5 scenario for each community, with non-emerging areas in gray (d, e, f) Relative climate change signal for each of the three communities, computed as the multi-member mean difference between the SSP5-8.5 fish biomass averaged over the 2070–2100 period and the historical biomass averaged between 1850 and 1900. The latter is also used to normalize the signal and represent it as a percentage.

(Figures 8e and 8f). Both communities demonstrate an emerging signal across extensive Pacific and Atlantic Oceans regions, particularly in areas exhibiting moderate to pronounced declines in fish biomass. Signals emerge in specific areas before 2020, including the northeastern Pacific, the equatorial Atlantic and the southeast of Madagascar. The projected signal patterns for the mesopelagic and migratory communities (Figures 8e and 8f) also demonstrate some resemblance to those of mesozooplankton (Figure 7d, pattern correlation of 0.60 with the mesozooplankton signal), indicating a likely bottom-up effect.

4. Discussion and Summary

4.1. Discussion

Our results indicate that climate change-induced biomass signals will emerge across 67%–74% of the ocean surface by the end of the century. An important question is whether mitigation policies can reduce regional emergence. Figure 9 compares the cumulative percentage of the emerging ocean surface for climate change signal

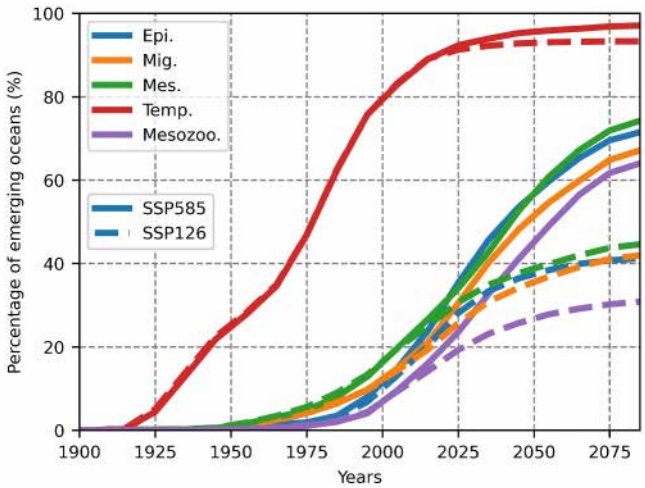

Figure 9. Cumulative percentage of the ocean surface in which the signal emerges for environmental variables and fish biomass in the SSP5-8.5 and the SSP1-2.6 scenarios.

in SST, mesozooplankton and fish biomass for both SSP5-8.5 and SSP1-2.6 scenarios. While mitigation policies marginally affect the ToE of SST (see also Figures S3 and S4 in Supporting Information S1), they significantly reduce the surface impacted by climate change for biological signals. By the end of the century, mesozooplankton will emerge across 31% of the ocean surface in the SSP1-2.6 scenario compared to 64% in the SSP5-8.5 scenario (Figure S5 in Supporting Information S1). Similarly, the biomass of epipelagic, migratory and mesopelagic fish will emerge in 41%, 42% and 45% of the ocean surface in the SSP1-2.6 scenario and 71%, 67% and 74% in the SSP5-8.5 scenario. This reduction is due to a deceleration in emergence from 2030 onwards (Figure S3 in Supporting Information S1), a consequence of the weaker climate change signal in the mitigated scenario (Figure S6 in Supporting Information S1). These results suggest that mitigation policies could maintain future marine ecosystems within the range of their natural variations in most oceanic regions. The differences in the response of global mean (Figure 2) and regional ToEs to mitigation result from the weaker noise in the former.

Our analysis also underscores the influence of the size class on the ToE. Both small (<1 cm) and large (>50 cm) epipelagic organisms exhibit earlier emergence than the intermediate organisms (about 20 cm). The later emergence of intermediate epipelagic organisms results from more prominent noise. In contrast, small migratory fish fail to emerge due to a weak signal, which strengthens with size, resulting in an early emergence of large organisms by 2025. For the mesopelagic community, interpreting the changes in ToE with size is more challenging because changes in signal and noise have opposite effects. Understanding the fish biomass changes due to natural variability and in response to climate change as a function of size is beyond the scope of this study. Still, it is a promising avenue for future research.

Additionally, significant uncertainties persist in the biogeochemical response to climate change across Earth System Models (ESMs, Bopp et al., 2022), leading to robust ToE for physical signals but less consistency for biogeochemical variables, including chlorophyll (Schlunegger et al., 2020). These uncertainties propagate into the fish biomass response to climate change (Tittensor et al., 2021), resulting in a ToE that might differ if another ESM was used to force APECOSM. Using a single Marine Ecosystem Model (MEM) is another limitation as projections of fish biomass response to climate change widely differ across MEMs (Tittensor et al., 2021). Assessing the impact of those uncertainties on the ToE of fish biomass would require performing ensemble simulations from multiple ESMs for the 9 MEM ensembles included in the Fisheries and Marine Ecosystem Model Intercomparison Project (FishMIP, Tittensor et al., 2018; Lotze et al., 2019; Tittensor et al., 2021). However, this requires significant computing and storage resources. Qualitatively, the global mean time series provided in Tittensor et al. (2021) suggests that models with the strongest signal (MACROECOLOGICAL, BOATS) and/or the weakest noise (DBPM, EcoOcean) will show early emergence compared to the other MEMs. APECOSM, which exhibits a comparatively moderate signal and substantial noise, may represent a higher-end ToE estimate.

Another limitation of this study is that we only considered the impact of climate change on the ecosystem without accounting for the effects of fishing, which also reduces fish biomass and may influence their ToE (Sibert et al., 2006). Recognizing this, the FishMIP community has developed the Ocean System Pathways (the OSPs, Maury et al., 2025) framework, derived from the SSPs and designed to project the combined spatio-temporal dynamics of fisheries and marine ecosystems. This framework will allow for exploring the impact of fisheries and climate change on the emergence of fish biomass changes and identifying potential synergies. OSPs could be used to address the additive effects of fishing on the emergence of marine ecosystems. This can be achieved through sensitivity experiments, similar to those by Heneghan et al. (2021), by fixing climate or fishing efforts at pre-industrial levels and comparing results with control and climate-change simulations where both factors vary.

4.2. Summary

This study represents the first attempt to estimate the Time of Emergence (ToE) of climate-driven changes in fish biomass. ToE refers to when these changes have or will emerge from the natural variability. Using ensemble climate-to-fish simulations based on the APECOSM ecosystem model forced with the IPSL-CM6A-LR Earth System Model physical and biogeochemical outputs, we determine the ToE of the epipelagic, migratory, and mesopelagic communities and their two main environmental drivers, temperature and mesozooplankton.

Globally averaged fish biomass signals emerge during the historical period for the epipelagic and mesopelagic communities but much later for the migratory ones (2036). The decline in fish biomass for the three communities mirrors mesozooplankton's, suggesting a bottom-up control of their response to climate change. However, the signal of epipelagic fish biomass emerges earlier (1950) than that of mesozooplankton (2001) due to a stronger signal in the early 20th century, likely related to trophic amplification induced by an early emerging surface warming (1915). Conversely, the trophic amplification for the mesopelagic community lags due to delayed warming in the mesopelagic zone (500–1,000 m), resulting in a later emergence (2017). The very weak signal for the migratory community (reduction of the global biomass of 4%) accounts for its late emergence.

Regional emergence lags behind global mean signals, except for the migratory fish biomass, for which the median of the regional ToE is consistent with the ToE of global mean biomass. For example, the peak of regional mesozooplankton emergence occurs 30 years later than that of the global mean mesozooplankton, 75 years for epipelagic and 30 years for the mesopelagic fish communities. This delay can be attributed to the considerably weaker noise of globally averaged biomass in comparison to the regional noise. Additionnally, our study shows that mitigation policies could strongly reduce the ocean surface where biogeochemical and biological signals emerge (about 70% in the SSP5-8.5 scenario and about 40% in the SSP1-2.6 scenario), although there is no effect of mitigation when considering global mean time-series.

Data Availability Statement

The data associated with this paper are available on Zenodo for the historical simulations and Seanoe for the climate change simulations. Due to storage limitations on Zenodo, each historical member is hosted on a single repository.

- hist-r14: Barrier (2024a) (https://doi.org/10.5281/zenodo.14047714)
- hist-r1: Barrier (2024b) (https://doi.org/10.5281/zenodo.14045797)
- hist-r2: Barrier (2024c) (https://doi.org/10.5281/zenodo.14046098)
- hist-r3: Barrier (2024d) (https://doi.org/10.5281/zenodo.14046127)
- hist-r4: Barrier (2024e) (https://doi.org/10.5281/zenodo.14046499)
- hist-r6: Barrier (2024f) (https://doi.org/10.5281/zenodo.14046489)
- ssp126, all members: Barrier (2024g) (https://doi.org/10.17882/102964)
- ssp585, all members: Barrier (2024h) (https://doi.org/10.17882/102974)

Software Availability: The Python scripts used to analyze the results and generate the figures are provided in Barrier et al. (2024) (https://zenodo.org/records/13734403).

Acknowledgments
The authors acknowledge the support from the European Union's Horizon 2020 research and innovation program under grant agreement No 817806 (TRIATLAS) as well as support from the French ANR project CIGOEF (Grant ANR-17-CE32-0008-01) and DREAM (Grant ANR-22-CE56-0002-01). The authors acknowledge the World Climate Research Programme, which, through its Working Group on Coupled Modelling, coordinated and promoted CMIP6. We thank the climate modelling groups for producing and making available their model output, the Earth System Grid Federation (ESGF) for archiving the data and providing access, and the multiple funding agencies that support CMIP6 and ESGF. The authors acknowledge the Pôle de Calcul et de Données Marines (PCDM, http://www.ifremer.fr/pcdm) for providing DATARMOR storage, data access, computation resources, visualisation and support services. The authors acknowledge Maelys Metge, who started this work as part of her internship. The authors acknowledge DeepL Write (https://www.deepl.com/write), which was used to improve the English in the manuscript.

References

Barrier, N. (2024a). APECOSM outputs used in the Earth's Future past and future of marine ecosystems [Dataset]. *Special Issue (Historical-r14)*. https://doi.org/10.5281/zenodo.14047714
Barrier, N. (2024b). APECOSM outputs used in the earth's Future past and future of marine ecosystems [Dataset]. *Special Issue (Historical-r1)*. https://doi.org/10.5281/zenodo.14045797
Barrier, N. (2024c). APECOSM outputs used in the Earth's Future past and future of marine ecosystems [Dataset]. *Special Issue (Historical-r2)*. https://doi.org/10.5281/zenodo.14046098
Barrier, N. (2024d). APECOSM outputs used in the Earth's future past and future of marine ecosystems [Dataset]. *Special Issue (Historical-r3)*. https://doi.org/10.5281/zenodo.14046127
Barrier, N. (2024e). APECOSM outputs used in the Earth's future past and future of marine ecosystems [Dataset]. *Special Issue (Historical-r4)*. https://doi.org/10.5281/zenodo.14046499
Barrier, N. (2024f). APECOSM outputs used in the Earth's future past and future of marine ecosystems [Dataset]. *Special Issue (Historical-r6)*. https://doi.org/10.5281/zenodo.14046489
Barrier, N. (2024g). Global fish biomass density under the IPSL-CM6-LR SSP1-2.6 climate change scenario for epipelagic, migratory and resident communities and 100 sizes ranging from 0.12cm to 1.96m [Dataset]. https://doi.org/10.17882/102964
Barrier, N. (2024h). Global fish biomass density under the IPSL-CM6-LR SSP5-8.5 climate change scenario for epipelagic, migratory and resident communities and 100 sizes ranging from 0.12cm to 1.96m [Dataset]. https://doi.org/10.17882/102974

Barrier, N., Lengaigne, M., Rault, J., Person, R., Ethé, C., Aumont, O., & Maury, O. (2023). Mechanisms underlying the epipelagic ecosystem response to ENSO in the equatorial Pacific ocean. *Progress in Oceanography*, *213*, 103002. https://doi.org/10.1016/j.pocean.2023.103002

Barrier, N., Maury, O., & Lengaigne, M. (2024). APECOSM Python scripts used in the Earth's Future [Software]. *Past and Future of Marine Ecosystems*. https://doi.org/10.5281/zenodo.13734403

Beaumont, L. J., Pitman, A., Perkins, S., Zimmermann, N. E., Yoccoz, N. G., & Thuiller, W. (2011). Impacts of climate change on the world's most exceptional ecoregions. *Proceedings of the National Academy of Sciences*, *108*(6), 2306–2311. https://doi.org/10.1073/pnas.1007217108

Bijma, J., Pörtner, H.-O., Yesson, C., & Rogers, A. D. (2013). Climate change and the oceans – What does the future hold? *Marine Pollution Bulletin*, *74*(2), 495–505. https://doi.org/10.1016/j.marpolbul.2013.07.022

Bopp, L., Aumont, O., Kwiatkowski, L., Clerc, C., Dupont, L., Ethé, C., et al. (2022). Diazotrophy as a key driver of the response of marine net primary productivity to climate change. *Biogeosciences*, *19*(17), 4267–4285. https://doi.org/10.5194/bg-19-4267-2022

Bopp, L., Resplandy, L., Orr, J. C., Doney, S. C., Dunne, J. P., Gehlen, M., et al. (2013). Multiple stressors of ocean ecosystems in the 21st century: Projections with CMIP5 models. *Biogeosciences*, *10*(10), 6225–6245. https://doi.org/10.5194/bg-10-6225-2013

Boucher, O., Servonnat, J., Albright, A. L., Aumont, O., Balkanski, Y., Bastrikov, V., et al. (2020). Presentation and evaluation of the IPSL-CM6A-LR climate model. *Journal of Advances in Modeling Earth Systems*, *12*(7), e2019MS002010. https://doi.org/10.1029/2019MS002010

Chavez, F. P., Messié, M., & Pennington, J. T. (2011). Marine primary production in relation to climate variability and change. *Annual Review of Marine Science*, *3*(1), 227–260. https://doi.org/10.1146/annurev.marine.010908.163917

de Luzinais, V. G., du Pontavice, H., Reygondeau, G., Barrier, N., Blanchard, J. L., Bornarel, V., et al. (2023). Trophic amplification: A model intercomparison of climate driven changes in marine food webs. *PLoS One*, *18*(8), e0287570. https://doi.org/10.1371/journal.pone.0287570

Deutsch, C. A., Tewksbury, J. J., Huey, R. B., Sheldon, K. S., Ghalambor, C. K., Haak, D. C., & Martin, P. R. (2008). Impacts of climate warming on terrestrial ectotherms across latitude. *Proceedings of the National Academy of Sciences*, *105*(18), 6668–6672. https://doi.org/10.1073/pnas.0709472105

Diaz, H. F., Hoerling, M. P., & Eischeid, J. K. (2001). ENSO variability, teleconnections and climate change. *International Journal of Climatology*, *21*(15), 1845–1862. https://doi.org/10.1002/joc.631

Diffenbaugh, N. S., & Scherer, M. (2011). Observational and model evidence of global emergence of permanent, unprecedented heat in the 20th and 21st centuries. *Climatic Change*, *107*(3), 615–624. https://doi.org/10.1007/s10584-011-0112-y

Faugeras, B., & Maury, O. (2005). An advection-diffusion-reaction size-structured fish population Dynamics model combined with a statistical parameter estimation procedure: Application to the Indian Ocean skipjack tuna fishery. *Mathematical Biosciences and Engineering*, *2*(4), 719–741. https://doi.org/10.3934/mbe.2005.2.719

Giorgi, F., & Bi, X. (2009). Time Of Emergence (TOE) of GHG-forced precipitation change hot-spots. *Geophysical Research Letters*, *36*(6). https://doi.org/10.1029/2009GL037593

Guiet, J., Aumont, O., Poggiale, J.-C., & Maury, O. (2016). Effects of lower trophic level biomass and water temperature on fish communities: A modelling study. *Progress in Oceanography*, *146*, 22–37. https://doi.org/10.1016/j.pocean.2016.04.003

Hawkins, E., & Sutton, R. (2012). Time of emergence of climate signals. *Geophysical Research Letters*, *39*(1). https://doi.org/10.1029/2011GL050087

Heneghan, R. F., Galbraith, E., Blanchard, J. L., Harrison, C., Barrier, N., Bulman, C., et al. (2021). Disentangling diverse responses to climate change among global marine ecosystem models. *Progress in Oceanography*, *198*, 102659. https://doi.org/10.1016/j.pocean.2021.102659

Heneghan, R. F., Hatton, I. A., & Galbraith, E. D. (2019). Climate change impacts on marine ecosystems through the lens of the size spectrum. *Emerging Topics in Life Sciences*, *3*(2), 233–243. https://doi.org/10.1042/ETLS20190042

Henson, S. A., Beaulieu, C., Ilyina, T., John, J. G., Long, M., Séférian, R., et al. (2017). Rapid emergence of climate change in environmental drivers of marine ecosystems. *Nature Communications*, *8*(1), 14682. https://doi.org/10.1038/ncomms14682

Hurrell, J. W., & Deser, C. (2009). North Atlantic climate variability: The role of the North Atlantic oscillation. *Journal of Marine Systems*, *78*(1), 28–41. https://doi.org/10.1016/j.jmarsys.2008.11.026

Keller, K. M., Joos, F., & Raible, C. C. (2014). Time of emergence of trends in ocean biogeochemistry. *Biogeosciences*, *11*(13), 3647–3659. https://doi.org/10.5194/bg-11-3647-2014

Koojman, S. (2010). Dynamic Energy Budget theory for metabolic organisation (3rd ed.).

Lefort, S., Aumont, O., Bopp, L., Arsouze, T., Gehlen, M., & Maury, O. (2015). Spatial and body-size dependent response of marine pelagic communities to projected global climate change. *Global Change Biology*, *21*(1), 154–164. https://doi.org/10.1111/gcb.12679

Lotze, H. K., Tittensor, D. P., Bryndum-Buchholz, A., Eddy, T. D., Cheung, W. W. L., Galbraith, E. D., et al. (2019). Global ensemble projections reveal trophic amplification of ocean biomass declines with climate change. *Proceedings of the National Academy of Sciences*, *116*(26), 12907–12912. https://doi.org/10.1073/pnas.1900194116

Maury, O. (2010). An overview of APECOSM, a spatialized mass balanced "Apex Predators ECOSystem Model" to study physiologically structured tuna population dynamics in their ecosystem. *Progress in Oceanography*, *84*(1), 113–117. https://doi.org/10.1016/j.pocean.2009.09.013

Maury, O. (2017). Can schooling regulate marine populations and ecosystems? *Progress in Oceanography*, *156*(Supplement C), 91–103. https://doi.org/10.1016/j.pocean.2017.06.003

Maury, O., & Poggiale, J.-C. (2013). From individuals to populations to communities: A dynamic energy budget model of marine ecosystem size-spectrum including life history diversity. *Journal of Theoretical Biology*, *324*, 52–71. https://doi.org/10.1016/j.jtbi.2013.01.018

Maury, O., Shin, Y.-J., Faugeras, B., Ben Ari, T., & Marsac, F. (2007). Modeling environmental effects on the size-structured energy flow through marine ecosystems. Part 2: Simulations. *Progress in Oceanography*, *74*(4), 500–514. https://doi.org/10.1016/j.pocean.2007.05.001

Maury, O., Tittensor, D., Eddy, T., Allison, E., Bahri, T., Barrier, N., et al. (2025). The Ocean System Pathways (OSPs): A new scenario and simulation framework to investigate the future of the world fisheries. *Earth's Future*, *12*.

O'Neill, B. C., Tebaldi, C., van Vuuren, D. P., Eyring, V., Friedlingstein, P., Hurtt, G., et al. (2016). The scenario Model Intercomparison Project (ScenarioMIP) for CMIP6. *Geoscientific Model Development*, *9*(9), 3461–3482. https://doi.org/10.5194/gmd-9-3461-2016

Pörtner, H.-O., & Peck, M. A. (2011). Effects of climate change. In *Encyclopedia of fish physiology: From genome to environment, Vols 1-3* (pp. 1738–1745). Elsevier Academic Press Inc.

Pörtner, H.-O., Roberts, D. C., Tignor, M., Poloczanska, E. S., Mintenbeck, K., Alegría, A., et al. (2022). Climate change 2022: Impacts, adaptation, and vulnerability. In *Contribution of working group II to the sixth assessment report of the intergovernmental panel on climate change (Tech. Rep.)*. IPCC.

Rodgers, K. B., Lin, J., & Frölicher, T. L. (2015). Emergence of multiple ocean ecosystem drivers in a large ensemble suite with an Earth system model. *Biogeosciences*, *12*(11), 3301–3320. https://doi.org/10.5194/bg-12-3301-2015

Santana-Falcón, Y., & Séférian, R. (2022). Climate change impacts the vertical structure of marine ecosystem thermal ranges. *Nature Climate Change*, *12*(10), 935–942. https://doi.org/10.1038/s41558-022-01476-5

Schlunegger, S., Rodgers, K. B., Sarmiento, J. L., Ilyina, T., Dunne, J. P., Takano, Y., et al. (2020). Time of emergence and large ensemble intercomparison for ocean biogeochemical trends. *Global Biogeochemical Cycles*, *34*(8), e2019GB006453. https://doi.org/10.1029/2019GB006453

Sibert, J., Hampton, J., Kleiber, P., & Maunder, M. (2006). Biomass, size, and trophic status of top Predators in the Pacific ocean. *Science*, *314*(5806), 1773–1776. https://doi.org/10.1126/science.1135347

Tittensor, D. P., Eddy, T. D., Lotze, H. K., Galbraith, E. D., Cheung, W., Barange, M., et al. (2018). A protocol for the intercomparison of marine fishery and ecosystem models: Fish-MIP v1.0. *Geoscientific Model Development*, *11*(4), 1421–1442. https://doi.org/10.5194/gmd-11-1421-2018

Tittensor, D. P., Novaglio, C., Harrison, C. S., Heneghan, R. F., Barrier, N., Bianchi, D., et al. (2021). Next-generation ensemble projections reveal higher climate risks for marine ecosystems. *Nature Climate Change*, *11*(11), 973–981. https://doi.org/10.1038/s41558-021-01173-9

Ying, J., Collins, M., Cai, W., Timmermann, A., Huang, P., Chen, D., & Stein, K. (2022). Emergence of climate change in the tropical Pacific. *Nature Climate Change*, *12*(4), 356–364. https://doi.org/10.1038/s41558-022-01301-z